Oxidation of Carbon Monoxide by Oxygen in Shock Waves

A. M. Dean and G. B. Kistiakowsky

Citation: The Journal of Chemical Physics **53**, 830 (1970); doi: 10.1063/1.1674066
View online: http://dx.doi.org/10.1063/1.1674066
View Table of Contents: http://scitation.aip.org/content/aip/journal/jcp/53/2?ver=pdfcov
Published by the AIP Publishing

Oxidation of Carbon Monoxide by Oxygen in Shock Waves

A. M. Dean and G. B. Kistiakowsky
Department of Chemistry, Harvard University, Cambridge, Massachusetts 02138
(Received 30 March 1970)

The oxidation of CO by O_2, with and without small amounts of added H_2, was investigated in very dilute mixtures with argon at about 5.4×10^{17} particles/cc total concentration. The reaction was followed in incident shock waves by measuring CO and CO_2 infrared emissions for about 2000 μsec particle time over the 1700–2600°K range. The reaction shows an initial accelerating rate followed, in H_2 mixtures, by a period of constant rate. The observed $[CO_2]$–time profiles were compared to those calculated numerically on an IBM 360/65 computer. These calculations used two branching-chain mechanisms proposed by others. The one involving hydrogenous impurities is

$$CO+O_2=CO_2+O, \quad (1)$$
$$O+H_2=OH+H, \quad (2)$$
$$O+H_2O=OH+OH, \quad (3)$$
$$OH+CO=CO_2+H, \quad (4)$$
$$OH+H_2=H_2O+H, \quad (5)$$
$$H+O_2=OH+O, \quad (6)$$

which describes all of the observations if the assumption is made that the total hydrogenous impurity (H_2 and H_2O) is approximately 40 ppm. This figure is in the range of the experimentally estimated impurity concentrations. In the calculations, least-squares averages of literature values of k_3, k_5, and k_6 were used and best fits were obtained with: $k_1=5.8\times10^{+12}\exp(-50\,000/RT)$ cc molecule^{-1}·sec^{-1}, $k_2=1.5\times10^{-10}\exp(-10\,000/RT)$ cc molecule^{-1}·sec^{-1}, $k_4=1.9\times10^{-12}\exp(-1030/RT)$ cc molecule^{-1}·sec^{-1}. With these values, which are consistent with literature data referring to high temperatures, quantitative agreement was obtained between calculated and observed rates of CO_2 formation. The observed rates could not be explained by the other proposed mechanism, which postulated electronically excited CO_2 as a chain carrier.

INTRODUCTION

The oxidation of carbon monoxide by molecular oxygen has been the object of numerous investigations.[1] Recently it was also studied in shock waves by several investigators.[2–4] These experiments have suggested that a chain-branching process is involved in the production of carbon dioxide. The same conclusion had been reached by earlier workers. Two mechanisms have been advanced to account for the shock-tube observations. Sulzmann, Myers, and Bartle[2] (SMB) have suggested that above 2400°K the chain branching is caused by electronically excited CO_2 molecules. However, Brokaw[5] has suggested that the chain branching in the SMB experiments proceeds via hydrogenous impurities. He was able to fit SMB's induction period data by assuming 20 ppm H_2O and a value for the rate constant for the reaction $O+H_2O=OH+OH$, which is the upper limit of those reported in the literature. However, SMB claimed to have only approximately 1 ppm of hydrogenous impurities. Fishburne, Bilwakesh, and Edse[3] report that their data can be explained by either of the above mechanisms if it is assumed that 7 ppm of H_2O were present.

In this investigation an attempt is made to distinguish between these two mechanisms by determining more experimental parameters. Data are presented on the reaction profile (approximately 0.1%–10% reaction) in addition to the induction times measured by other workers.[2,4] Several mixtures with added H_2 were also studied; here the H_2 concentration was large enough for the total concentration of hydrogenous species to be accurately determined. A numerical integration routine was used to calculate $[CO_2]$-vs-time profiles using each of the proposed mechanisms. Calculations using Brokaw's mechanism compared very favorably with the data.

EXPERIMENTAL

The 3-in.-i.d. shock-tube, ir detector system, and gas-handling apparatus, as well as the method of temperature calculation and data collection, have all been described previously.[6] In the present work helium was used as the driver gas. Infrared emission was observed at 4.20 and 5.03 μ behind incident shock waves in CO/O_2 and $CO/O_2/H_2$ mixtures highly diluted with argon. The half-height bandpass was 0.18 μ for the 4.20 μ filter and 0.14 μ for the 5.03-μ filter. A variable delay unit was installed for the triggering of the oscilloscopes and two dual-trace Tektronix 1A1 plug-in units were used. Each signal was divided and displayed on both oscilloscopes, which were set at different sensitivities and sweep speeds. The 4.20 μ signal was used to follow the production of CO_2, while the 5.03 μ signal measured CO emission. The CO vibrational relaxation time was comparable to the time scale of these experiments; the CO signal was initially

TABLE I. Summary of experimental conditions.

Mixture	%CO	$\%O_2$	$\%H_2$	CO density (10^{16} molecules/cc)	Temp. range (°K)
1	4.26	2.08	···	2.24–2.36	1765–2245
2	4.24	2.07	···	2.27–2.35	2070–2110
3	8.50	4.20	···	4.62–4.94	1735–2450
4	4.31	2.13	···	2.30–2.47	2240–2575
5	4.17	2.10	0.0175	2.20–2.34	1750–2575
6	4.27	2.08	0.0495	2.31–2.37	1730–2580
7	4.22	2.08	···	2.22–2.34	2100–2140

zero and increased to an equilibrium value during the observation time. A small signal was observed at 4.20 μ when CO/Ar mixtures were shocked. Therefore several CO/Ar mixtures were shocked to determine the correction factor to be applied to the 4.20 μ signal during reactive shocks. It was possible to relate this correction at a given time to the magnitude of the CO signal at the same time during the reactive shock of interest. Several CO_2/Ar mixtures were also shocked over the temperature range of interest to determine the 4.20 μ sensitivity for CO_2. It was established that the 4.20 μ signal was directly proportional to CO_2 concentration over the range observed in the reactive shocks. Additional CO_2 calibration shocks were done intermittently during the course of the experiments; the sensitivity of the detector system thus continually checked was found to remain constant to within 5% at a given temperature. The reaction was typically followed for approximately 2000 μsec of particle time in incident shocks. Consideration was given to the possibility that boundary layer growth might make the ideal shock assumptions invalid at long observation times. Such boundary layer effects would tend to increase the temperature and density of the gas as well as make the ideal relation between particle time and lab time invalid.[7] However, the increase in temperature and density would both tend to increase the emission from CO_2; the fact that the observed CO_2 emission in calibration shocks was found to remain constant for periods of time longer than the observation periods in reactive shocks was taken to indicate that ideal shock conditions could be maintained. Thus in this work the particle time was computed in the usual way. Estimates of background pressure of impurities were obtained by multiplying the measured outgassing rate in the evacuated unfilled tube by the time elapsed between closure of the pump valve followed by the introduction of the gas mixture and the initiation of the shock wave. This time interval was normally approximately 1 min. The preshock pressure of all mixtures was 4.5–4.7 torr. Other experimental conditions are summarized in Table I.

In these experiments both Matheson research-grade and C. P. grade carbon monoxide were used. This C. P. CO was the same supply used in an earlier work.[8] At that time it had been analyzed with a CEC 21—103*C* mass spectrometer and no appreciable impurities had been observed. However, recent data with a different supply of CO revealed large decreases in the rate of CO_2 production and in the vibrational relaxation rate of CO. The C.P. CO was then distilled at 77°K, and the final 5% fraction was analyzed in a Bendix time-of-flight mass spectrometer and revealed significant concentrations of impurities. It was not possible to quantitatively analyze this sample; the main peaks that could not be assigned to CO were at $m/e=15$, 31, 44, 45, 46, and 60. Much smaller peaks at 56 and 84 might be assigned to iron carbonyl. Thus CO for these experiments was passed very slowly through a packed trap at 77°K before use. In the earlier work it was thought best not to attempt any purification since this might produce some variance in the trace concentrations of CO_2 and thus affect the correction factor. When it became evident that this CO supply contained appreciable reactive impurities and must be purified, CO/Ar calibration shocks were done whenever a new supply of CO was introduced into the vacuum line. This precaution proved unnecessary as the correction factor remained invariant for a given grade of CO. Matheson research-grade and extra-dry-grade oxygen were used without further purification. Airco research-grade argon and Matheson prepurified-grade hydrogen were used throughout. This argon was analyzed on a CEC 21–103C mass spectrometer; no H_2 or H_2O was observed, with the detection limit for H_2 being approximately 15 ppm.

RESULTS

A typical CO_2 profile is plotted in Fig. 1, and the three regions to be discussed in this paper are indicated.

Induction Time (t_i)

This was defined as the particle time when the CO_2 concentration reached 1.6×10^{13} molecules/cc. Physi-

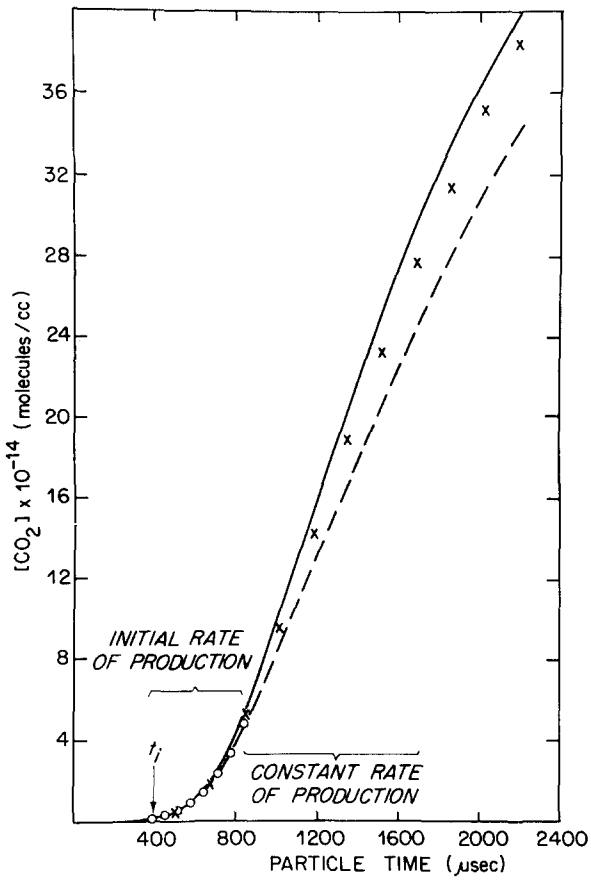

FIG. 1. Typical plot of $[CO_2]$ vs time. Mixture 5, $T=2155°K$, $\rho_{CO}=2.32\times10^{16}$ molecules/cc, background pressure $=1.3\times10^{-4}$ torr. O, readings from first scope; ×, readings from second scope. Solid line is the calculated profile using Set 2 as input; dashed line is calculated from Set 3 (see text).

cally this concentration represents the minimum signal at 4.20 μ which could be reproducibly extracted from the noise. The observed induction times are shown in Fig. 2. These are not directly comparable with those of SMB because of a different definition of the induction time. The background pressure in the shock tube, calculated as described above, varied in these runs from 3×10^{-5} to 5.5×10^{-4} torr. This variation was obtained by changing the pump-down times of the shock tube and thus the measured outgassing rates. These changes in the background pressure had no statistically detectable effect on measured induction times. Note in Fig. 2(a) that the t_i values at lower temperatures exhibit a very small dependence on $[CO]$ and $[O_2]$. An increase of a factor of 2 in both $[CO]$ and $[O_2]$ decreases t_i by less than a factor of 2 at temperatures less than 1900°K. Such comparisons cannot be made at the highest temperatures since it was not possible to obtain valid data on t_i at temperatures greater than 2400°K. In this region the induction time came sufficiently early such that the errors involved in determining the correction factor became too large. At these early times (and low signals) the ratio of signals at 4.20 and 5.03 μ in CO/Ar shocks could not be adequately determined. However, it is apparent from Fig. 2(a) that the dependence of t_i on $[CO]$ and $[O_2]$ increases as the temperature is increased. Figure 2 also indicates that the temperature dependence of t_i increases at higher temperatures for runs with no added H_2, while no such increase is evident in runs with added H_2.

Initial Rate of Production of CO_2

Accelerating Rate

The profiles of $[CO_2]$ vs time of all mixtures indicated that the rate of production of CO_2 increased with increasing time during the early stages of the reaction (with the exceptions noted below). Plots were made of $\log[CO_2]$ vs time to see if this increase was exponential. A particular run was said to fit if the experimental data fell on a straight line over at least a decade of CO_2 concentration growth. All runs with added H_2 gave good fits on these semilog plots; the slopes (λ') of these plots are shown in Fig. 3. At temperatures less than 2400°K all runs with no added

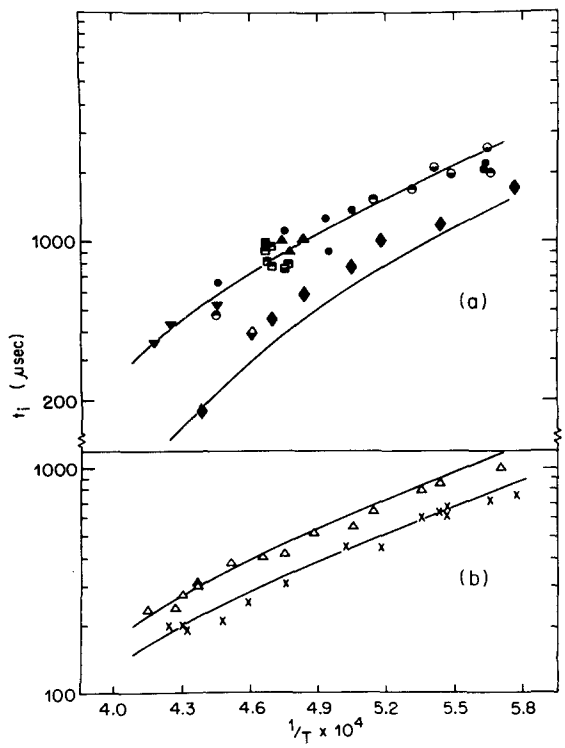

FIG. 2. Plots of induction times t_i vs $1/T$. (a) Mixtures with no added H_2. Solid symbols indicate that the background pressure (P_{bg}) is in the range $1.0-2.0\times10^{-4}$ torr. Symbols with the upper half solid indicate $3.3\times10^{-4}\leq P_{bg}\leq5.5\times10^{-4}$. Symbols with the lower half solid indicate $3\times10^{-5}\leq P_{bg}\leq6\times10^{-5}$. ●, Mixture 1; ▲, Mixture 2; ▼, Mixture 4; ■, Mixture 7; here $\rho_{CO}\sim2.3\times10^{16}$ molecules/cc. Solid diamond, Mixture 3; here $\rho_{CO}\sim4.8\times10^{16}$ molecules/cc. (b) Mixtures with added H_2. △, Mixture 5 (175 ppm H_2); ×, Mixture 6 (495 ppm H_2). Solid lines are calculated values of t_i (see text).

H_2 in which it was possible to observe a decade of $[CO_2]$ increase (i.e., those runs where the CO_2 concentration was greater than 1.6×10^{14} molecules/cc at the end of the observation period) also exhibited exponential growth. λ' for these runs are shown in Fig. 4. At temperatures greater than 2400°K, semilog plots of these mixtures tended to be concave downward, particularly for the 8% CO mixture. The data in Fig. 4 have two very interesting features: (1) With one exception the rate of exponential increase in mixtures with 4% CO appears related to the background

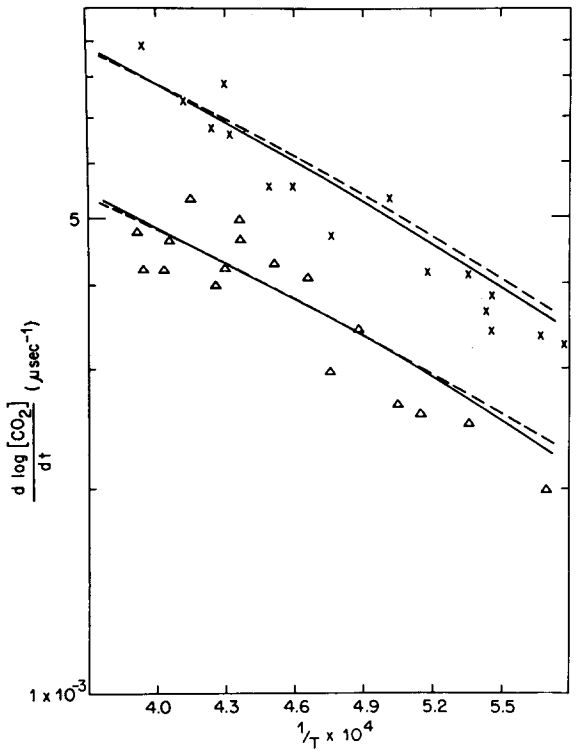

FIG. 3. Plots of exponential growth constants λ' ($\lambda'=d\log[CO_2]/dt$) vs T^{-1} for mixtures with added H_2. △, Mixture 5; ×, Mixture 6. Solid lines are calculated values using Set. 2. Dashed lines used the values in Set 3.

pressure. (2) The dependence of λ' on [CO] and $[O_2]$ is very low. At 2100°K, doubling both [CO] and $[O_2]$ results in an increase of approximately 50% in λ'. This behavior is very similar to the effect of [CO] and $[O_2]$ on t_i at lower temperatures.

Initiation Reaction

In mixtures with no added H_2, all shocks at temperatures greater than 2200°K had a region of linear CO_2 production before the observed acceleration in rate occurred. In these shocks, the first three or four data points extrapolated to the origin on a plot of $[CO_2]$ vs time. For shocks above 2400°K, this behavior was evident after the initial data point had

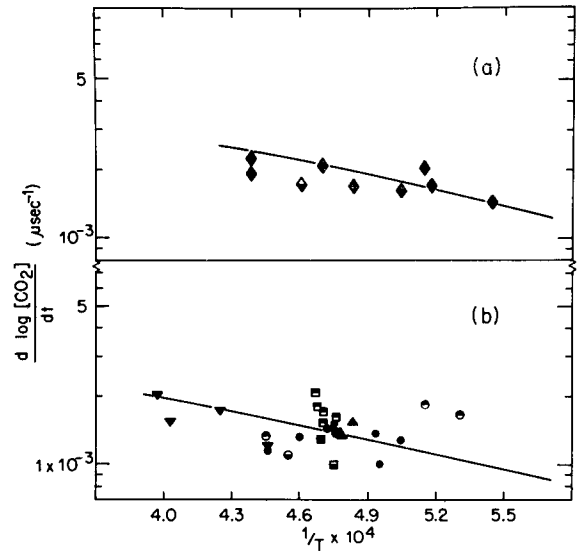

FIG. 4. Plots of λ' vs $1/T$ for mixtures with no added H_2. (a) $\rho_{CO}\sim4.8\times10^{16}$ molecules/cc. (b) $\rho_{CO}\sim2.3\times10^{16}$ molecules/cc. Labeling is the same as Fig. 2. Solid lines are calculated values of λ' assuming 20 ppm H_2 and 20 ppm H_2O. Values of k_2 and k_4 are specified by Set 2 (see text).

been disregarded for the reasons discussed in the t_i section. This initial constant rate of CO_2 production was presumably caused by the "initiation reaction." Previous workers[2,5] had suggested that this reaction was

$$CO+O_2=CO_2+O, \qquad (1)$$

and we defined k_1 as the value of the initial rate

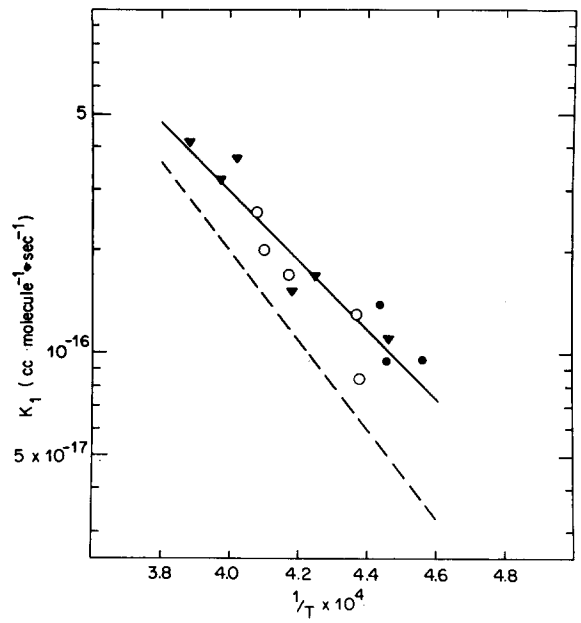

FIG. 5. Arrhenius plot of k_1 $\{k_1=(d[CO_2]/dt)_i([CO][O_2])^{-1}\}$. ●, Mixture 1; ○, Mixture 3; ▼, Mixture 4. Solid line is a least-squares fit to the directly observed values of k_1. The dashed line indicates the value of k_1 which gave the best fit to induction period data.

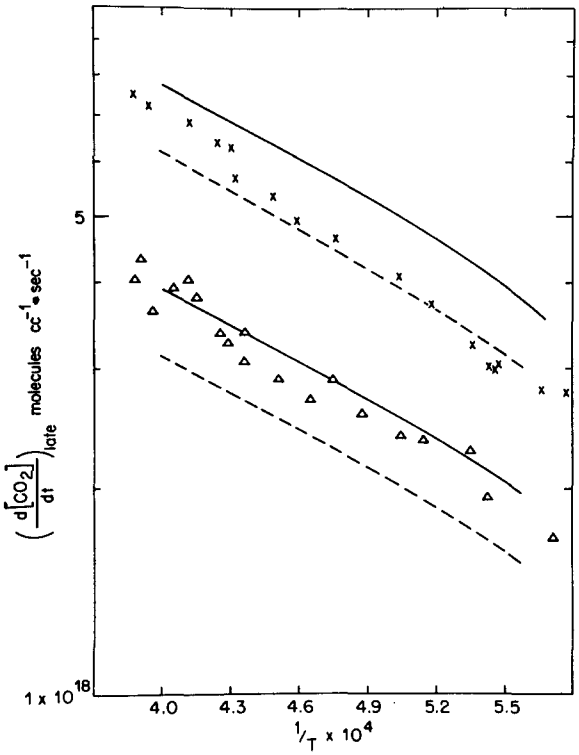

FIG. 6. Plots of constant (late) rates of CO_2 production vs T^{-1} for runs with added H_2. △, Mixture 5; ×, Mixture 6. Solid lines are the calculated values using Set 2. Dashed lines are calculated using Set 3 (see text).

divided by the concentrations of CO and O_2. An Arrhenius plot of k_1 is shown in Fig. 5. A least-squares fit to the data in Fig. 5 gave

$$k_1=(3.0\pm0.8)\times10^{-12}\exp[(-45\,600\pm2700)/RT]$$

in units of centimeter^3 molecule^{-1}·second^{-1}.

Constant (Late) Rate of CO_2 Production

Mixtures with added H_2 manifested regions of constant CO_2 production later in the reaction. This region typically began after several percent of the CO had been converted to CO_2. These constant rates are shown in Fig. 6. In all experiments with no added H_2 the rates of CO_2 production were still accelerating even near the end of the observation period.

DISCUSSION

As indicated in the Introduction, two mechanisms have been proposed for the shock-tube oxidation of CO by O_2. In an attempt to resolve this conflict we have calculated profiles of $[CO_2]$ vs time using each of these schemes. These calculated profiles were then compared to our experimental observations.

Consideration of Brokaw's "Impurity Mechanism"

The possible reactive impurities in our experiments could come from two sources. The first would be those which were present in either CO, O_2, or argon. Mixture 1 contained research-grade CO and O_2, while Mixture 2 contained C.P. CO and extra-dry O_2. The rates of CO_2 production were identical in these mixtures; this was taken to mean that neither the CO (purified as described in the Experimental section) nor O_2 contained appreciable reactive impurities. This leaves argon as the most likely source of impurities. The mass-spectrometric analysis indicates that the argon might contain up to 15 ppm H_2, although this is well above the 1 ppm level of H_2 claimed by Airco. A second source of contamination was the outgassing products of the shock tube. If this outgassing rate were the same when the mixture was added as in the evacuated tube, the water concentration (presumably a large fraction of the outgassing) at the time of a typical shock might be as high as 30–40 ppm. The fact that λ' in Fig. 4(b) is related to the background pressure indicates that this is a significant source of impurities. Thus it would seem that the typical impurity levels for these experiments might be set at approximately 1–15 ppm H_2 and 30–40 ppm H_2O.

Brokaw[5] has postulated that CO_2 production in CO/O_2 mixtures without added hydrogen could be explained by trace amounts of hydrogenous impurities (H_2 or H_2O). His scheme consists of the reactions

$$CO+O_2=CO_2+O, \quad (1)$$

$$O+H_2=OH+H, \quad (2)$$

$$O+H_2O=OH+OH, \quad (3)$$

$$OH+CO=CO_2+H, \quad (4)$$

$$OH+H_2=H_2O+H, \quad (5)$$

$$H+O_2=OH+O. \quad (6)$$

Assuming no depletion of CO, O_2, H_2, or H_2O and neglecting back reactions, he derived expressions for the exponential growth constant (λ) and for CO_2 production. λ was shown to be the positive root of

$$\phi^3+(v_2+v_3+v_4+v_5+v_6)\phi^2+[v_3v_6+(v_2+v_3)(v_4+v_5)]\phi-2v_6(v_2+v_3)(v_4+v_5)=0 \quad (A)$$

and

$$[CO_2]=v_1\left[\frac{v_4}{v_4+v_5}\left(\frac{\sinh\lambda t}{\lambda}+\frac{\cosh(\lambda t)-1}{v_6}\right)+\frac{v_5 t}{v_4+v_5}\right], \quad (B)$$

where $v_1=k_1[CO][O_2]$, $v_2=k_2[H_2]$, $v_3=k_3[H_2O]$, $v_4=k_4[CO]$, $v_5=k_5[H_2]$, and $v_6=k_6[O_2]$.

A numerical integration routine kindly supplied by Gardiner and Walker[9] was modified and programmed for an IBM 360/65 computer[10] to calculate $[CO_2]$-vs-time profiles using Brokaw's reaction scheme and the accompanying back reactions so that the validity of (A) and (B) might be checked. Using the same initial concentrations and rate constants, induction times

TABLE II. Values used for rate constants [$k=A\exp(-E/RT)$ cc molecule^{-1}·sec^{-1}].[a]

Reaction	A	E	Comments and Refs.
(2) $O+H_2=OH+H$	1.0×10^{-10}	10.0 kcal/mole	"Standard"; Ref. 11
(3) $O+H_2O=OH+OH$	6.3×10^{-10}	19.5	Ref. 5
(4) $OH+CO=CO_2+H$	1.1×10^{-12}	1.0	"Standard"; Ref. 12
(5) $OH+H_2=H_2O+H$	6.3×10^{-11}	5.5	Ref. 12
(6) $H+O_2=OH+O$	4.2×10^{-10}	16.8	Ref. 12

[a] All reverse reaction rate constants were calculated from the values of the equilibrium constants. Equilibrium constants were computed from *JANAF*.

determined from these profiles agreed very well with the values obtained using (A) and (B). In addition to an enormous decrease in required computer time, Brokaw's calculational method has another advantage: (B) predicts that at times sufficiently long for terms in $\exp(-\lambda t)$ to be neglected and yet short enough so that the reactants have not been significantly depleted, the CO_2 concentration will rise approximately exponentially with growth constant λ. Thus the solution of (A) will yield a positive root λ which can be directly related to the observed exponential growth rates,

$$d\log[CO_2]/dt=\lambda/2.303=\lambda'. \qquad (C)$$

This approximation has been compared to the numerical integration routine and found to be valid to within approximately 5%. Thus (A) and (B) can be used to calculate t_i and λ' to a very good degree of approximation.

Calculation of λ'

Attempts were first made to calculate λ' from (A) for the mixtures which contained added H_2. Here the concentration of H_2 was sufficiently great relative to our estimated levels of impurities that these calculations were quite insensitive to small variations (i.e., 20 ppm or so) in our assumed concentrations of impurities. The initial rate constants used for this calculation were taken from the literature and are shown in Table II. Browne, White, and Smookler's[11] value of k_2 was chosen since this seemed to be the most reliable high-temperature value in the sense that their density profiles were quite sensitive to k_2. Brokaw's[5] value of k_3 was used; calculations for mixtures with added H_2 are insensitive to the value of k_3. Schofield's[12] suggested value for k_4 is a least-squares fit over the temperature range 300–2000°K and depends mainly on data at temperatures lower than those in this work. The rate constants k_5 and k_6 are least-squares fits that encompass the temperature range of these experiments. The results of these calculations indicated that this set of rate constants gave insufficient branching to account for our observations. It was shown that λ' is most sensitive to k_2 and k_4, and these rate constants were then varied in an attempt to fit our data. The following combinations of values of k_2 and k_4 gave quite good fits to our data on λ':

Set	k_2	k_4
1	Standard (Table II)	Standard (Table II)$\times3$
2	Standard$\times\frac{4}{3}$	Standard$\times2$
3	Standard$\times\frac{5}{3}$	Standard$\times\frac{3}{2}$.

The calculated values using Sets 2 and 3 are shown in Fig. 3.

Now these values of rate constants were used to calculate λ' for the mixtures with no added H_2. Here the variable was the impurity concentration. These concentrations were systematically varied, and the best fit was obtained assuming 20 ppm H_2 and 20 ppm H_2O. Calculations assuming 5 ppm H_2 and 40 ppm H_2O indicated a similar dependence of λ' on [CO] and [O_2], but the temperature dependence using this set of impurities was larger. When using 20 ppm H_2 and 20 ppm H_2O, the calculated λ' was very similar for all three sets of k_2 and k_4 values. The fit using Set 2 is shown in Fig. 4. Thus it appears that the concentrations of impurities we might expect in our system could explain the observed exponential growth rates. It should be emphasized that the assignment of impurities as 20 ppm H_2 and 20 ppm H_2O is quite arbitrary. Given the scatter of the data and the uncertainty in the value of k_3, other combinations such as 10 ppm H_2 and 30 ppm H_2O are capable of describing the data. Our main point is that the total concentrations of hydrogeneous impurities that might be present in these experiments is capable of generating sufficient CO_2 to explain the observations. Perhaps the most striking aspect of this calculation is the excellent agreement regarding the small dependence of λ' on the concentrations of CO and O_2.

Calculation of t_i

With this agreement between calculated and observed exponential growth rates it was possible to calculate t_i under the constraint that the only variable was k_1. The t_i calculations were done assuming 20 ppm H_2 and 20 ppm H_2O as impurities. This combination reproduced the observed temperature dependence of λ', and this was essential in any t_i calculation. The λ' calculations indicate that significant branching is oc-

curring in mixtures with no added H_2, and especially at low temperatures this contributes significantly to the production of CO_2 even before time t_i. Only with the proper temperature dependence of the branching process can one determine the proper temperature dependence of the initiation reaction. These t_i calculations gave an independent value of k_1 to compare to the directly observed value discussed earlier. For the calculations described here, the values of k_2 and k_4 specified in Set 2 were used. Use of the other sets gave similar results. The best fit to all mixtures was obtained with the following:

$$k_1 = 3.5\times10^{-11}\exp(-60\,000/RT) \text{ cc molecule}^{-1}\cdot\text{sec}^{-1}.$$

This fit is shown in Fig. 2, and Fig. 5 compares this value with that directly observed. The agreement is within a factor of 2 over the temperature range 2200–2600°K, and the "direct" values might be high since they include some small contribution from branching reactions. The average value of k_1 over a temperature range 2200–2600°K (see Fig. 5) is

$$k_1 = 5.8\times10^{-12}\exp(-50\,000/RT) \text{ cc molecule}^{-1}\cdot\text{sec}^{-1}.$$

This can be compared to the value of $5.8\times10^{-12}\times\exp(-51\,000/RT)$ cc molecule$^{-1}\cdot$sec^{-1} reported in the earlier shock-tube investigation by Sulzmann, Myers, and Bartle.[2]

These results on k_1 are probably in some diasgreement with earlier work done in this laboratory. A study[13] of the exchange reaction $^{18}O+C^{16}O=C^{18}O+{}^{16}O$ indicated that the concentration of oxygen atoms was approximately 30 times higher than would be predicted by SMB's value of k_1. An investigation[14] of the $O+CO_2=CO+O_2$ reaction yielded a value for k_{-1} over an order of magnitude larger than would be calculated from the SMB value of k_1 and $K_{eq}(1)$. Unreasonably high levels of inpurities must be postulated in these two studies to account for such a large discrepancy in the value of k_1. Thus the disparity between the TOF results[13,14] and the ir emission results of this work and SMB's experiments remain unexplained.

Perhaps the most interesting aspect of these calculations is the marked effect of such small amounts of impurities. In runs without added H_2, the curvature of the t_i plots indicates the increasing dominance of the branching process as the temperature is decreased and the same is demonstrated by the small dependence of t_i on $[CO]$ and $[O_2]$ at lower temperatures.

The calculations on λ' and t_i also qualitatively explain why no regions of exponential growth were observed at the highest temperatures in mixtures with no added H_2. Here the high-activation-energy initiation reaction produces significant concentrations of CO_2, and the increase of $[CO_2]$ with time could not be described exclusively by an exponential term. The marked effect of background pressure on λ' but not on t_i can be similarly explained. λ' is characteristic of the chain-branching reactions and thus would be affected by an increase in the concentration of H_2O. However, the initiation rate is important at the earliest observed times and this would tend to obscure the background pressure effect on t_i. This is particularly true in light of the fact that the most intensive study of the effect of background pressure was done at the relatively high temperature of approximately 2125°K. Thus all of our observations on the initial accelerating rate of CO_2 production in CO/O_2 and $CO/O_2/H_2$ systems can be described by Brokaw's mechanism.

Calculation of Constant (Late) Rates of CO_2 Production

The next step was to use the average value of k_1 in conjunction with the sets of rate constants which successfully described t_i and λ' in an attempt to calculate the observed constant rates of CO_2 production later in the reaction for mixtures with added H_2. In this region the numerical integration routine must be used since Eqs. (A) and (B) are no longer valid. Reactions (1)–(6) predict an increase in atomic-oxygen concentration closely paralleling $[CO_2]$. Thus the calculated profiles included the reaction

$$CO+O+M=CO_2+M. \qquad (7)$$

The reported rate constants for this reaction have varied over orders of magnitude.[15] The value chosen for these calculations was an average of the values reported by shock-tube workers in a similar temperature range,[16,17]

$$k_7 = 1.6\times10^{-34} \text{ cc}^2 \text{ molecule}^{-2}\cdot\text{sec}^{-1}.$$

The rate of CO_2 production via Reaction (7) was never larger than 1% of the rate via Reaction (4) with this value of k_7. Thus our results are not sensitive to the value of k_7.

Preliminary profile calculations indicated that the reverse reactions (−2), (−3), (−5), and (−6) became significant at the end of the exponential growth period resulting in a relatively constant concentration of OH radicals in the system which is only slightly affected by using different sets of k_2 and k_4. This constant $[OH]$ accounts for the observed constant CO_2 production since in this region all of the CO_2 can be considered to be produced via Reaction (4). Thus the rate of CO_2 production is approximately proportional to k_4, which should distinguish between the various sets of k_2 and k_4 which gave good fits to λ'. Set 1 gave significantly larger rates than were observed and further calculations were done with Sets 2 and 3. The calculated values for these sets are shown in Fig. 6. The complete profiles for Mixture 5 at 2150°K using both sets of rate constants are compared to an experimental profile in Fig. 1. The agreement is most encouraging. It would seem

from Fig. 6 that a set of values of k_2 and k_2 intermediate between Sets 2 and 3 would describe most of observed constant rates within 10%. These intermediate values which would seem most consistent with all of our data are

$$k_2 = 1.5\times10^{-10}\exp(-10\,000/RT) \text{ cc molecule}^{-1}\cdot\text{sec}^{-1},$$

$$k_4 = 1.9\times10^{-12}\exp(-1030/RT) \text{ cc molecule}^{-1}\cdot\text{sec}^{-1}.$$

It should be noted that all variations of rate constants tried involved the pre-exponential factors. The reported activation energies for these reactions were determined over a much wider range of $1/T$ than in the present work, and changes in E did not seem justified.

In summary, it appears that the mechanisms consisting of Reactions (1)–(6) is quantitatively capable of describing our entire reaction profile. This profile, which typically extended well over two orders of magnitude of $[CO_2]$ increase, demonstrates an initial exponential rise of OH and CO_2 followed by a pseudo-equilibrium of [OH] which results in a constant rate of production of CO_2.

Chain Branching via CO_2*

Although (1)–(6) describe the observations in both CO/O_2 and $CO/O_2/H_2$ systems, consideration was also given to the possibility that the excited CO_2 mechanism[2] might account for the observed branching in systems with no added H_2. This mechanism can be expressed in its simplest form as

$$CO+O_2=CO_2+O, \quad (1)$$

$$CO+O+(M)=CO_2^*+(M), \quad (8)$$

$$CO_2^*+O_2=CO_2+O+O, \quad (9)$$

where CO_2* indicates electronically excited CO_2. Clyne and Thrush[18] have proposed that CO_2* is a triplet with a binding energy of approximately 40 kcal/mol. Unfortunately, the reactions in this scheme have not been studied extensively and the rate constants are matters of conjecture.

Brokaw[5] has considered this system and has shown that the value of k_{-8} needed to fit SMB's data is much smaller than that obtained from equilibrium constant considerations of reactions analogous to (8).[19] We used Brokaw's equation for the exponential growth constant in this scheme and his estimate of $K_{eq}(8)$ in an attempt to fit our observed λ'. Again, his solution was tested by the numerical integration of this system of equations and was found to be valid. Brokaw shows that

$$\lambda\sim k_8k_9[CO][O_2]/(k_8[CO]+k_{-8}+k_9[O_2]). \quad (D)$$

Under the conditions of these experiments, use of Brokaw's estimate of $K_{eq}(8)$ predicts $k_8[CO]\ll k_{-8}$. Also, k_9 will probably have a much higher activation energy than k_8, and then $k_9[O_2]\ll k_{-8}$. Thus,

$$\lambda\sim k_8k_9[CO][O_2]/k_{-8}, \quad (E)$$

and this is in marked contrast to the experimental results that λ' ($=\lambda/2.303$) showed very little dependence on [CO] and $[O_2]$. Alternatively, use of Eq. (D) to fit λ' would result in a value for the pre-exponential factor of k_9 several orders of magnitude above collisional. This latter argument was used by Brokaw to show that SMB's data could not be explained by this mechanism. Thus it would appear that the observed branching in mixtures with no added H_2 cannot be explained by the CO_2* mechanism.

CONCLUSION

Our intent in this work was to attempt to resolve the questions concerning the mechanism of CO oxidation. We have shown that our results strongly favor Brokaw's "impurity mechanism." The data in systems with no added H_2 can be explained by concentrations of impurities which are comparable to estimated impurity levels. However, the specific concentrations which gave the best fit cannot be considered an unambiguous assignment, and these data cannot be used to estimate reliable values for either k_2 or k_3. The work in systems with added H_2 is not limited in this respect, as regards k_2. Here the concentration of H_2 is well above our impurity estimates, and the only variables under these conditions are the rate constants themselves. Data on λ' is most sensitive to k_2 and k_4, and the constant rate of production of CO_2 in these mixtures is very sensitive to k_4. In this light, the values of k_2 and k_4 can be specified quite well by calculated fits to the data. The reported best fit of k_4 compares quite favorably to other high-temperature determinations of this rate constant.[15] The k_2 value determined here is a factor of 1.5 higher than that reported in recent work.[11]

Of particular interest in the k_2 determination is the higher sensitivity of a low $[H_2]$ system to this chain-branching reaction relative to a system containing stoichiometric amounts of H_2 and O_2. An analogous approach will be used to study chain-branching reactions in hydrocarbon–oxygen systems. Hopefully this will complement recent studies in which stoichiometric mixtures of oxygen and hydrocarbons were used. The potential advantage of our approach is that the technique of numerical integration allows quantitative study of various stages of the reaction. In particular, one is not limited to such small extents of conversion as were demanded by earlier methods of computing profiles, and consequently for the reaction here described more definite assignments of rate constants became possible.

ACKNOWLEDGMENTS

The authors wish to thank the Office of Naval Research for funds which made this research possible.

One of us (A. M. D.) wishes to thank the National Science Foundation for its support of his graduate work.

[1] G. J. Minkoff and C. F. H. Tipper, *Chemistry of Combustion Reactions* (Butterworths, London, 1962).
[2] K. G. P. Sultzmann, B. F. Myers, and E. R. Bartle, J. Chem. Phys. **42**, 3969 (1965); **43**, 1220 (1965).
[3] E. S. Fishburne, K. R. Bilwakesh, and R. Edse, Aerospace Res. Labs. Rept. ARL 67-0113, May 1967.
[4] L. J. Drummond, Australian J. Chem. **21**, 2631 (1968).
[5] R. S. Brokaw, Symp. Combust. 11th Berkeley, 1966, 1063 (1967).
[6] J. B. Homer and G. B. Kistiakowsky, J. Chem. Phys. **46**, 4213 (1967); **47**, 5290 (1967).
[7] R. L. Belford and R. A. Strehlow, Ann. Rev. Phys. Chem. **20**, 247 (1969).
[8] A. M. Dean and G. B. Kistiakowsky, Tech. Rept. Office of Naval Research, Contract Nonr-1866(36), September 1969 (unpublished).
[9] B. F. Walker, Ph.D. thesis, University of Texas, 1968.
[10] A. M. Dean, Tech. Rept. Office of Naval Research, Contract Nonr-1866(36), September 1969.
[11] W. G. Browne, D. R. White, and G. R. Smookler, Symp. Combust. 12th, Poitiers, 1968, 557 (1969).
[12] K. Schofield, Planetary Space Sci. **15**, 643 (1967).
[13] S. H. Garnett, G. B. Kistiakowsky, and B. V. O'Grady, J. Chem. Phys. **51**, 84 (1969).
[14] T. C. Clark, S. H. Garnett, and G. B. Kistiakowsky, J. Chem. Phys. **51**, 2885 (1969).
[15] D. L. Baulch, D. D. Drysdale, and A. C. Lloyd, "High Temperature Reaction Rate Data," University of Leeds, (1968), No. 1.
[16] T. A. Brabbs and F. E. Belles, Symp. Combust. 11th, Berkeley, 1966, 125 (1967) (as quoted by Ref. 15).
[17] H. A. Olschewski, J. Troe, and H. Wagner, Symp. Combust. 11th, Berkeley, 1966, 155 (1967) (as quoted in Ref. 15).
[18] M. A. A. Clyne and B. A. Thrush, Symp. Combust. 9th Ithaca, 1963, 177 (1964).
[19] Brokaw estimates $K_{eq}(-8)=7\times10^{4}\ \exp(-E/RT)$ mol liter^{-1} at 1597°K. (E is the CO_2* binding energy.)

THE JOURNAL OF CHEMICAL PHYSICS VOLUME 53, NUMBER 2 15 JULY 1970

Energy-Level Scheme for Nd^{3+} in $LiYF_4$*

D. SENGUPTA AND J. O. ARTMAN†
Department of Physics, Carnegie-Mellon University, Pittsburgh, Pennsylvania 15213

(Received 12 January 1970)

Crystal-field parameters appropriate for S_4 symmetry were fit to existing data on the $^4I_{9/2}$ and $^4I_{11/2}$ sublevel splittings of $LiYF_4$:Nd^{3+}. Intermediate coupling wavefunctions obtained previously from fits to the $CaWO_4$:Nd^{3+} spectrum were used. Although ground-state EPR data were not available in this system, the symmetries of the levels were uniquely assignable from group-theoretical considerations and the available polarization data. The parameter values found are (in cm^{-1}): $B_0^2=482.7$, $B_0^4=-1452.5$, $B_0^6=-122.1$, $B_4^4=-1222.0$, $B_4^6=-981.9$, $B_4'^4=-0.3$, and $B_4'^6=-0.2$. The rms deviation of this fit was 10. We calculate ground-state $g_{\|}$ and $g_{\perp}$ values of 0.483 and 2.571, respectively. The crystal-field parameters found here are compared with those of $CaWO_4$:Nd^{3+} and those of the "mirror" ion Er^{3+} in $LiYF_4$:Er^{3+}. We conclude that simple geometrical considerations as to the algebraic signs of the crystal-field components in these systems may be misleading.

Polarized optical absorption and fluorescence data were taken on the Nd^{3+}:$LiYF_4$ system by Harmer, Linz, and Grabbe.[1] These researchers pointed out many similarities between these fluorescent spectra and those for Nd^{3+} in the isomorphous host $CaWO_4$. However, they did not perform a crystal-field analysis of the level splittings. In view of the close correspondence energy-wise between these two systems we have adapted a simplified version of our Nd^{3+}:$CaWO_4$ analysis[2] to the present case.

Harmer and co-workers established the electric dipole nature of the radiation, however, they did *not* assign the symmetries to the various crystal-field split levels. In view of the radiation selection rules for S_4 symmetry[3] only *relative* Γ_6, Γ_7 designations can be established immediately from the optical observations. In such cases the Γ assignment of the ground state is determined usually by comparison of the calculated g value with experiment and then the other assignments automatically follow. However, pertinent EPR data do not seem to be available for this system. Fortunately the results of group theory can extract us from our dilemma. The polarization characteristics of the $^4F_{3/2}\rightarrow{}^4I_{9/2}$ fluorescence were clear; also *all* the expected transitions were found. A $J=\frac{9}{2}$ level must break up into three Γ_7 levels and two Γ_6 levels in S_4 symmetry.[4] The *proper* assignment of symmetries to the $^4I_{9/2}$, $^4I_{11/2}$, and $^4F_{3/2}$ components for Nd^{3+}:$LiYF_4$ corresponds indeed to the Nd^{3+}:$CaWO_4$ case[2] (see Fig. 1). The alternate incorrect assignment would lead to *two* Γ_6 levels and *three* Γ_7 levels in the $^4I_{9/2}$ multiplet; this is untenable.

The free-ion wavefunctions[5] derived in our previous Nd^{3+}:$CaWO_4$ work were used. These correspond to E^1, E^2, E^3, and ζ values of 4859.7, 24.78, 482.0, and 873.8, respectively (in cm^{-1}). The results of a fit (not including J–J mixing) to the $J=\frac{9}{2}$ and $J=\frac{11}{2}$ multiplet splittings are shown in Table I. (The rms deviations are comparable to our results in the $CaWO_4$ system.[6]) The crystal-field parameters used in this fit are entered in row A of Table II. The Nd^{3+}:$CaWO_4$ parameter values are listed in row B of this table. The values of the dominant parameters, except B_0^2, are somewhat